RSC Advances

ROYAL SOCIETY OF CHEMISTRY

www.rsc.org/advances

Biomilling of Rod-Shaped ZnO Nanoparticles: A Potential Role of *Saccharomyces cerevisiae* Extracellular Proteins

Chandrashekhar Sharan[1,2], Puneet Khandelwal[1,2], and Pankaj Poddar*[1,2,3]

[1]*Physical & Material Chemistry Division, CSIR-National Chemical Laboratory, Pune – 411008, India,*

[2]*Academy of Scientific and Innovative Research, Anusandhan Bhawan, 2 Rafi Marg, New Delhi-110 001,*

[3]*Center of Excellence on Surface Science, CSIR-National Chemical Laboratory, Pune – 411008, India*

Abstract

There is a tremendous interest in newly-discovered, green, room-temperature, biological routes for the fabrication of biologically-benign functional nanostructures. The bottom-up biogenic synthesis, where the precursor molecules form crystalline solids at nanoscale by redox process, has been validated over the years and gained its popularity. However, a new top-down technique that is recently developed in our group, in which, the small isotropic nanoparticles (NPs) are formed by the break-down of chemically-synthesized anisotropic rod or plate-shaped NPs using microbes (termed as biomilling). This technique, which holds great promise, is still in its infancy. Here, an improved process with an easy isolation of NPs from biomass and a better control over technique is reported. This novel technique is demonstrated to break-down the chemically synthesized ZnO nanorods (NRs), ~ 250 nm in length, to small quasi-spherical ZnO NPs (~ 10 nm in diameter) possibly due to the proteins secreted by the yeast (*Saccharomyces cerevisiae*), which also lead to formation of the "corona" around NPs. The UV-vis, PL and FTIR results show the dynamic nature of the protein corona, which is

further supported by the SDS-PAGE study of the extracellular proteins. The SDS-PAGE study of the intracellular proteins shows the over-expression of a single protein which is supposed to have a role in zinc transport in the cells. The ICP-OES results show the accumulation of higher amount of zinc in the yeast cells as biomilling progresses, while the extracellular zinc content were almost same. Therefore, we believe that the yeast cells play an important role in biomilling process by secreting the proteins and maintaining the zinc content in the extracellular fluid. The biomilled NPs exhibit uniform dispersibility and enhanced aqueous stability than chemically synthesized ZnO NRs.

Key words: Biomilling, top-down synthesis, biosynthesis, zinc-oxide nanoparticles, *S. cerevisiae*, yeast, protein-corona

Introduction

Despite of proven advancement in the chemical and physical methods for the synthesis of various nanomaterials, there is still a concern due to the use of toxic chemicals, high temperature and pressure etc. However, considering the sustainability in future, there is always a demand to develop green chemistry methods to synthesize the nanomaterials, which are energy-efficient, and environment friendly. Nature always inspires with new sustainable, energy-efficient, self-replicating and eco-friendly ideas, whether it is biomimetic engineering,[1,2] bio mineralization,[3] bioleaching,[4-5] bioremediation,[6] or biotransformation.[7] Two different approaches have been used for the synthesis of nanoparticles (NPs) (1) bottom-up; in which, the NPs are synthesized from their precursor molecules and, (2) Top-down; in which, the bigger particles are broken-down to the nanoscale size by the physical methods such as ball-milling, laser ablation[8] etc. Among these two approaches, the bottom-up approach has been extensively used by bionanotechnologists for the biosynthesis of metal[9,10] and metal oxide[11] NPs from their precursors. However, there was no previous report on the biological synthesis of NPs using top-down method until the recent work reported by our group.[12-13]

In our first report, we demonstrated the synthesis of very small NPs (< 10 nm) by the break-down of chemically synthesized BiOCl particles, much larger in size, using biological approach and we termed it, for the first time, as "biomilling".[12] In our next study, the biomilling of chemically-synthesized $BaTiO_3$ micro-scaled particles using yeast (*S. cerevisiae*) biomass was also reported.[13] However, as any other new process, the biomilling, being in its infancy, requires new ideas. Moreover, it is full of challenges that require a lot of efforts until this novel process reaches its maturity and becomes industrially feasible. Some

of the challenges are (1) easier isolation of biomilled NPs from the biomass, (2) understanding the biochemical mechanism of biomilling, and (3) scaling-up the process.

In this study, we chose the yeast *S. cerevisiae* as a model system to study the biomilling of the ZnO nanorods (NRs) because *S. cerevisiae* is highly tolerant to metal ions,[14] and it is also known for its ability to accumulate certain metal ions such as zinc, copper and manganese, through various physico-chemical processes.[15] At least 31 % of yeast genes have homologs in the human genome[16]. Moreover, the complete genome and proteome database is readily available.[17] *S. cerevisiae* has been utilized since ancient times for the production of bread and bear etc., and is considered to be safe for human consumption.[18] Therefore, biomilled NPs can be used for drug delivery because it is the nanoparticle–corona complex rather than the bare nanoparticles which interact with biological system, and in accord to that, can change the fate of NPs in the living systems.[19, 20]

ZnO is well known for its unique properties such as piezoelectricity,[21] UV absorbance,[22] sensitivity to gases and chemical agents,[23] catalysis[24] etc. These unique properties lead to an extensive applicability of this material for solar-photovoltaic,[25-28] piezoelectric-transducers,[29] short-wavelength lasers,[30] phosphors,[31] light emitting diodes[32] etc. Recently, ZnO is proved to be an excellent material for the biological applications such as antimicrobial agents,[31] UV-protectants in sunscreen lotions, cancer treatment[34,35] etc.

There are many methods available in the literature for the synthesis of ZnO NPs such as sol-gel,[36] simple solution combustion method,[37] chemical vapor synthesis,[38] hydrothermal method,[39] microwave assisted synthesis of microcrystals,[40] microwave assisted hydrothermal synthesis of nanowires,[41] and laser ablation.[8] However, the green top-down biological method to synthesize ZnO NPs is not reported so far. As yeast cells are endowed with various biomolecules that could potentially break-down the larger particles, the biomilling technique efficiently utilizes these cells for the synthesis of protein-capped quasi-spherical ZnO NPs.

Here, we report the biomilling of chemically-synthesized ZnO NRs (~ 250 nm in length) to demonstrate the synthesis of very small, protein-capped, quasi-spherical ZnO NPs (~ 10 nm in diameter). Here, efforts are made to address some of the challenges associated with the biomilling process reported by our group recently.[12-13] The modified biomilling procedure developed by us in this report, has several inherent advantages over our earlier reported work as we demonstrate that it is possible to (1) isolate the biomilled NPs with minimum efforts, (2) separate the top-down biomilling and bottom-up biosynthesis processes (if the organism itself, has NP synthesis ability by extra/intracellular reduction of free zinc ions to form NPs), and (3) differentiate the yeast cell involvement in the biomilling process. Detailed experimental investigation proves the formation of well-crystalline, small-sized protein-capped, quasi-spherical ZnO NPs after nearly 168 h of biomilling. The UV-vis, photoluminescence (PL) and FTIR spectroscopic studies as a function of biomilling-time, show the dynamic nature of protein corona on the ZnO NPs, which is further supported by the SDS-PAGE analysis of the extracellular fluid. We believe that the yeast cells provide an important role in the process of biomilling by accumulating a high amount of zinc content in the cells while the zinc content in extracellular medium almost same as shown by the ICP-OES analysis. The biomilled ZnO NPs show enhanced stability and improved dispersibility in aqueous medium than chemically synthesized ZnO NRs.

Experimental section

Materials

All chemicals were of analytical grade and used as-received without any further purification, unless otherwise described. Dextrose monohydrate (AR grade), mycological peptone (certified), yeast extract powder (type I), malt extract powder were purchased from Himedia Laboratories. Dialysis tubing cellulose membrane (average flat width 33 mm, D 9652) was purchased from Sigma-Aldrich. Sodium hydroxide pellets (GR grade) were purchased from

Merck. Zinc acetate dehydrate [($Zn(CH_3COO)_2 \cdot 2H_2O$), extra pure, AR grade] was purchased from Sisco Research Laboratory Pvt. Ltd. All glassware were washed with aqua-regia (HCl/HNO_3 = 3:1) carefully and were rinsed with double-distilled water before being used in the reaction.

Chemical synthesis of ZnO NRs

The rod-shaped ZnO NPs were synthesized according to a method described in a previous report.[42] Briefly, zinc acetate and sodium hydroxide were dissolved in double-distilled water in the stoichiometric ratio and were stirred for ~ 45 min at room temperature (RT) followed by the hydrothermal reaction in a stainless steel vessel with Teflon liner at ~ 120 °C for ~ 24 h. The resultant material was washed several times with ethanol and water to remove the ionic impurities and dried in a vacuum oven for 6 h at 60 °C to result in a white powder.

Biomilling of chemically synthesized ZnO NRs

The chemically synthesized ZnO NRs were introduced to the yeast culture for a period of 168 h. For this purpose, the budding yeast *S. cerevisiae* (NCIM No. 3064) was sourced from National Collection of Industrial Microorganisms (NCIM) at CSIR-National Chemical Laboratory, Pune, India. The culture was grown in a 500 mL Erlenmeyer flask containing 150 mL of the MGYP medium (0.45 g malt extract, 0.45 g yeast extract, 0.75 g mycological peptone, and 1.5 g dextrose). The above flask was incubated at 28 °C under constant shaking at 150 rpm. After 48 h of growth, at late log phase, cells were harvested by centrifugation at 5000 rpm for 5 min at 4 ^{o}C. The cells were washed thrice and resuspended in autoclaved normal saline. The yeast cells were then transferred to a sterile Erlenmeyer flask. In this flask, a dialysis bag (molecular weight cutoff ~ 14 kDa) containing ZnO NRs (10 mg) dispersed in 15 mL double distilled water was added. The flask containing the cells along with the dialysis-bag was kept for incubation in a rotary shaker at 150 rpm for 168 h at 28 °C. The biomilling of ZnO NRs was monitored by withdrawing the biomilled ZnO NPs samples

from the dialysis bag at an interval of 24 h for a period of 168 h. The whole procedure was performed, aseptically, in a laminar air-flow cabinet. The biomilled NPs were characterized by UV-vis, fluorescence, Fourier transformed infrared spectrophotometer (FTIR), powder X-ray diffraction (XRD), transmission electron microscopy (TEM), and atomic force microscopy (AFM).

Characterization techniques

The particle morphology of the ZnO NPs was characterized by TEM and AFM. TEM images were recorded using a Tecnai F30 TEM instrument from FEI Inc. equipped with a field-emission source operating at 300 kV with S-TWIN objective lens and C_S value of 1.2 mm. The point resolution of the microscope was 0.24 nm. The sample was drop-casted on a carbon-coated copper grid with mess-size of 200 μm and air-dried in vacuum before being introduced into the TEM instrument. The AFM imaging was performed using a Multimode scanning probe microscope equipped with a Nanoscope IV controller from Veeco Instrument Inc., Santa Barbara, CA. For AFM imaging, the sample was drop-casted on the silicon-wafer and dried in vacuum. All the AFM measurements were done under ambient conditions using the tapping-mode AFM using Tap190Al AFM Budget Sensors® probes purchased from Innovative Solutions Bulgaria Ltd. The radius of curvature of tips used in this study was < 10 nm, and their height was 17 μm. The cantilever used had a resonant frequency of ca. 162 kHz and nominal spring constant of ca. 48 N/m with a 30 nm thick aluminum reflex coating on the backside of the cantilever of length 225 μm. For each sample, three locations with a surface area of 1 × 1 μm^2 each were imaged at a rate of 1 Hz and a resolution of 512 × 512 pixels. Powder X-ray diffraction (PXRD) patterns were obtained to confirm the synthesis of crystalline phases in the biomilled ZnO NPs. PXRD patterns were recorded by using a PHILIPS X'PERT PRO instrument equipped with X'celerator, a fast solid-state detector. Iron-

filtered Cu-K_α radiation (λ = 1.5406 Å) was used. The samples were drop-casted on a glass substrate. The XRD patterns were recorded in the 2θ range of 30 - 75°.

UV-visible and photoluminescence spectroscopic studies were conducted to analyze the optical properties of the biomilled ZnO NPs. Absorbance spectra were recorded using a Jasco UV-vis dual-beam spectrometer (Model V570) operated at a resolution of ~ 2 nm. Fluorescence emission spectra were recorded using a Cary Eclipse photoluminescence spectrophotometer from Varian equipped with a xenon flash lamp. Binding study of proteins on the surface of biomilled ZnO NPs was performed by FTIR. FTIR spectra were obtained using a Perkin Elmer Spectrum One instrument. The spectrometer operated in the transmission mode at a resolution of 4 cm^{-1}. The samples for FTIR studies were mixed with KBr powder and allowed to dry and the dried powder was directly used for FTIR studies.

In order to reveal the extracellular and intracellular protein expression profile as a function of biomilling time, 1D sodium dodecyl sulphate - polyacrylamide gel electrophoresis (SDS-PAGE) (18%) was performed. The cells were harvested by centrifugation at 5000 rpm for 5 min at 4 ^oC, washed twice with normal saline. The intracellular protein was extracted from cells by using SDS and β-mercaptoethanol treatment. From the cell supernatant, the extracellular protein was extracted by precipitation with trichloroacetic acid (TCA). The protein samples were mixed in 1:1 ratio with 2X loading buffer containing 4 % SDS and 8 % β-mercaptoethanol, were boiled for 5 min before loading to SDS-PAGE. We used standard molecular weight marker M3913, obtained from Sigma Aldrich.

Inductively coupled plasma - optical emission spectroscopy (ICP-OES) was used to analyze the extracellular as well as intracellular zinc content as a function of biomilling time. For extracellular zinc content, the samples taken during biomilling were centrifuged at 10,000 rpm for 15 min at 4 ^oC. The as-obtained supernatant was collected and filtered by nylon membrane filter paper with pore size of 0.2 μm before measuring the zinc content. The

experiment was performed in duplicates. To analyze the intracellular zinc content, a modified method of Demirci[43,44] was used for sample preparation. Briefly, the *S. cerevisiae* cells were harvested by centrifugation at 5000 rpm for 5 min at 4 ^{o}C. The cells were washed twice with normal saline solution and allowed to dry. The cell dry mass of 100 mg were taken in a long neck flask and 5 mL of conc. nitric acid was added and heated to 160 °C. Then, 2 mL of conc. sulphuric acid was added to it. To maintain the oxidizing environment, small amount of nitric acid was added till the solution gets colorless. After cooling-down to RT, the deionized water was added to make the final volume 50 mL. The content was filtered with 0.2 μm pore size nylon membrane before measuring the zinc content by ICP-OES, model Spectro Arcos (ARCOS-FHS-12) from SPECTRO Analytical Instruments GmbH.

Thermogravimetric analysis (TGA) experiments were carried-out in the temperature range of 25 - 750 °C on a SDT Q600 TG-DTA analyzer under N_2 atmosphere at a heating rate of 10 °C min^{-1}. A PALS Zeta Potential Analyzer Ver 3.54 (Brookhaven Instrument Corps.) was used to determine the electrophoretic mobilities. The mobilities were converted to zeta potential (ζ) using the Smoluchowski model.

Results and discussion

In order to visualize the effect of biomilling on the morphology and crystallinity of ZnO NPs, detailed TEM, AFM, and XRD studies were performed on the biomilled ZnO NP samples collected at an interval of 24 h for a period of 168 h. From the TEM image in figure 1a, the presence of well-defined rods with an average diameter of ~ 45 nm and an average length of ~ 250 nm were observed. It was noticed from figure 1b that after 24 h of biomilling, the ZnO NRs were fully covered with a thick amorphous protein layer and the rods as a whole and specifically, at the edges, started to break-down and an overall reduction in length and diameter of rods was observed. As the biomilling time was increased to 72 h, the average size of the ZnO NRs was decreased (figure 1c). After 120 h of biomilling (figure 1d), the

spherical NPs were found to coexist with a significantly reduced population of smaller size of ZnO NRs. Further, the presence of uniformly distributed very small quasi-spherical NPs with size ~ 10 nm was found in the TEM image of 168 h of biomilled NPs (figure 1e). The Zn, C, N and O elements were found in the corresponding Energy-dispersive X-ray spectrum (EDS) (figure 1f). AFM results were also confirmed the synthesis of very small spherical NPs with diameter ~ 10 nm (figure 2).

To study the effect of biomilling on crystalline quality and crystalline phases of chemically synthesized ZnO NPs, PXRD measurements were performed on biomilled ZnO NP samples collected at different time intervals, and presented in figure 3. The prominent peaks situated at 2θ values of 31.6°, 34.2°, 36.1°, 47.3°, 56.3°, 62.7°, 66.2°, 67.5° and 68.8° correspond to the (100), (002), (101), (102), (110), (103), (200), (112) and (201) planes, respectively, and can readily be indexed to hexagonal wurtzite structure of ZnO (JCPDS card no 36-1451). There was no significant change found in the relative peak intensities upon comparison of various XRD patterns. This was due to the fact that, not all the rod-shaped particles got biomilled into smaller quasi-spherical particles and partially-biomilled/completely un-biomilled particles present in the sample may still contributes to the XRD signals.

The effect of biomilling on the optical properties of ZnO NPs was studied by detailed UV-vis absorption and fluorescence emission spectroscopy measurements on the biomilled ZnO NPs taken out at a time interval of 24 h for a period of 168 h. The time-dependent changes in the UV-vis absorption spectra of the ZnO NPs after biomilling were shown in figure 4. It was noticed that most of the spectra show three characteristic features in the UV-vis range: (1) a broad absorption in the UV range centered at ~ 265 nm due to the π-π* transition in the aromatic amino acids containing coronal proteins,[45] (2) ~ 374 nm characteristic signature of ZnO NPs due to excitonic transition at room temperature,[46,47] and

(3) ~ 400 nm (Soret band) due to the π-π* transition in porphyrin containing proteins.[48] The observed small shift in the ~ 265 nm peak with biomilling time was attributed to the dynamic nature of proteins binding to the ZnO NPs. Moreover, a small shift in the ~ 374 nm peak as a function of biomilling time was also observed which can be related to the change in the dielectric environment due to the change in the composition of coronal proteins.[49] The shift in ~ 374 nm peak with change in the size of particles cannot be attributed to the quantum size effect, because the mean diameter of particles after biomilling was ~ 10 nm, which was higher than the reported excitonic Bohr diameter for ZnO (~ 6.5 nm).[50]

Further, the ratio of absorbance ~ 374 nm and ~ 265 nm ($A_{374/265}$) was used to assess the relative concentration of ZnO NPs with respect to the concentration of proteins in the biomilled samples. It was observed that the ZnO NPs concentration with respect to protein concentration, was increased almost linearly with time (figure 4 inset). The PL and FTIR results further supported the dynamic nature of coronal proteins (Supporting Information, Figure S1 and S2). TGA analysis indicated the presence of protein corona on the biomilled ZnO nanoparticles (Supporting Information, Figure S3).

In order to gain deeper insight in to the mechanism of biomilling process, SDS-PAGE and ICP-OES analysis were performed to determine the intracellular and extracellular protein expression profile and aqueous zinc content in the cell and extracellular fluid, respectively, as a function of biomilling time. To study the expression profile of extracellular and intracellular proteins secreted by yeast, *S. cerevisae* in the absence and presence of ZnO NPs as a function of biomilling time, SDS-PAGE analysis was performed. The expression profile of extracellular proteins in the absence and presence of ZnO NPs after every 48 h of time period such as 24 h, 72 h, 120 h and 168 h was shown in figure 5. It was observed that in presence of ZnO NPs, most of the proteins found to be under expressed. However, after 72 h of

biomilling, two proteins with M.W. ~ 6.5 kDa and ~ 30 kDa were found to be over expressed. Furthermore, after 120 h of biomilling, only one protein with M.W. ~ 39 kDa was found which was consistently present throughout the biomilling process and became more prominent at 168 h of biomilling. The expression profile of intracellular proteins in the absence and presence of ZnO NPs after every 48 h of time period was shown in the figure 6. It was observed from the figure 6, that a protein with M.W. ~ 30 kDa showed increase in the expression with biomilling time and assumed to be related to the zinc transport in the yeast cells as zinc transporter.

In order to analyze the change in concentration of extracellular and intracellular zinc content as a function of biomilling time, ICP-OES measurements were performed and presented in figure 7. It was noticed from the figure 7 that at 0 h, zinc content in the extracellular fluid was found almost negligible whereas, it was ~ 1 mg/L for intracellular zinc content. After 24 h, the extracellular zinc content was increased to ~ 0.25 mg/L and remains almost constant up to 72 h. However, in the same time, the intracellular zinc content was continuously increased to ~ 18.4 mg/L. After 96 h, the extracellular zinc content was increased by 10 times to ~ 2.75 mg/L and can be related to the release of zinc from the cells which lead to decrease in the intracellular zinc content to ~ 14.5 mg/L. The intracellular zinc content was further decreased to its minimum level ~ 6.9 mg/L. However, the exact reason behind the decrease in the intracellular zinc content is not known. It was observed that after 120 h, the extracellular zinc content was further decreased to ~ 1.25 mg/L and ~ 0.75 mg/L for 144 h of biomilling. Therefore, it is concluded that in the course of biomilling, yeast cells maintain the zinc content almost same in the extracellular fluid.

It is known that the yeast *S. cerevisiae* secretes a fair amount (few μg/mL) of proteins in the extracellular medium[51] which was also observed in our SDS-PAGE study. Some of these extracellular proteins may get attached to the positively charged ZnO NRs by

electrostatic interaction and can form the protein corona. The change in the surface charge from ~ +12.3 mV for chemically synthesized NRs (at 0 h) to ~ -29.5 mV (after 24 h) for biomilled ZnO NPs was observed in our zeta potential study (figure S4) which indicates the attachment of proteins to the surface of ZnO NPs. These proteins may act as chelating agents and leach-out the zinc ions. The leached-out ions can be taken up by yeast cells and stored in the vacuole, as it is the major site for zinc storage in the yeast cells.[52] The yeast *S. cerevisiae* is very well studied organism for zinc transport and trafficking.[53] This was also evident from our ICP-OES study that a higher amount of zinc content present inside the cells as compared to the extracellular zinc content. Therefore, we believe that the yeast cells play an important role in the biomilling by secreting the proteins as well as maintaining the zinc content almost same in the extracellular fluid throughout the biomilling process (scheme 1).

The dispersibility of the biomilled ZnO NPs in the aqueous medium was compared with the chemically synthesized ZnO NRs and was shown in figure 8. After 2 h, the absorbance at 374 nm was decreased by 10% for the biomilled ZnO NPs and 80% for chemically synthesized ZnO NRs. Further, the stability of both NPs suspension was compared at different time periods and biomilled ZnO NPs were found to be highly stable in aqueous suspension for a long time (figure 8, inset).

Conclusion

We have successfully developed a modified-biomilling process to transform the chemically synthesized ZnO NRs to protein-capped quasi-spherical ZnO NPs at room temperature in a process spontaneously driven by *S. cerevisiae* as a stress response. Detailed time-dependent TEM and XRD studies have indicated the formation of quasi-spherical ZnO NPs with the size ~ 10 nm, and it has further confirmed by AFM study. UV-vis, PL and FTIR studies have shown the dynamic nature of protein corona as a function of biomilling time. Zeta potential

study exhibited the abrupt change in the surface charge onto the NPs from ~ +12.3 mV (for chemically synthesized NRs, at 0 h) to ~ -29.5 mV (for biomilled ZnO NPs, after 24 h) which indicated the adherence of negatively charged protein molecules to the positively charged surface of ZnO NRs by electrostatic forces and formation of multiple layers of proteins. TGA analysis has also supported the presence of protein molecules with the biomilled ZnO NPs. The time dependent extracellular and intracellular protein expression profile by SDS-PAGE analysis has shown the over-expression of three different extracellular proteins with M.W. ~ 6.5 kDa, ~ 30 kDa and ~ 39 kDa; and one intracellular protein with M.W. ~ 30 kDa (assumed to be related to the zinc transport in the yeast cells), at different stages of biomilling. Moreover, the ICP-OES study has shown the accumulation of higher amount of zinc inside the cells in comparison to the extracellular fluid. Therefore, it is supposed that the yeast cells play an important role in biomilling by secreting the proteins as well as maintaining the zinc content almost same as in the extracellular fluid. Moreover, the biomilled ZnO NPs have shown higher dispersibility and stability in aqueous medium than chemically synthesized ZnO NRs. However, there is further scope to explore the exact mechanism behind the biomilling process and the fate of biomilled nanoparticles upon interaction with biological systems. It is believed that this study will be of great potential applications in biology field because of its green biological approach and ability to synthesize water dispersible and stable protein-capped quasi-spherical ZnO NPs.

Acknowledgement

P. P. acknowledges support from the Department of Science and Technology (DST), India (DST/INT/ISR/P-8/2011). P. P. also acknowledges support from CSIR network program on NANO-Safety, Health & Environment (NANO-SHE) and CSIR center of excellence on surface science. C.S. and P.K. acknowledge the support from the University Grant

Commission (UGC), India and the Department of Biotechnology (DBT), India for providing the Senior Research Fellowships, respectively.

References

1. R. Naik, S. Stringer, G. Agarwal, S. Jones and M. Stone, *Nature Materials*, 2002, 1, 169-172.
2. C. Tamerler and M. Sarikaya, *Acta Biomaterialia*, 2007, 3, 289-299.
3. K. Simkiss and K. Wilbur, *Biomineralization, Academic Press, New York,*1989.
4. C. Solisio, A. Lodi and F. Veglio, *Waste Management*, 2002, 22, 667-675.
5. V. Bansal, D. Rautaray, A. Ahmad and M. Sastry, *Journal of Materials Chemistry*, 2004, 14, 3303-3305.
6. A. Sanyal, D. Rautaray, V. Bansal, A. Ahmad and M. Sastry, *Langmuir*, 2005, 21, 7220-7224.
7. V. Bansal, A. Ahmad and M. Sastry, *Journal of the American Chemical Society*, 2006, 128, 14059-14066.
8. Y. Chung and W. Kang, *Journal-Korean Chemical Society*, 2006, 50, 440.
9. P. Khandelwal, D. K. singh, S. Sadhu, P. Poddar, *Chempluschem*, 2014, 79, 134-142.
10. D. K. Singh, R. Jagannathan, P. Khandelwal, P. M. Abraham and P. Poddar, *Nanoscale*, 2013, 5, 1882-1893.
11. Z. Tian, J. Voigt, J. Liu, B. McKenzie, M. McDermott, M. Rodriguez, H. Konishi and H. Xu, *Nature Materials*, 2003, 2, 821-826.
12. B. Mazumder, I. Uddin, S. Khan, V. Ravi, K. Selveraj, P. Poddar and A. Ahmad, *Journal of Materials Chemistry*, 2007, 17, 3910-3914.
13. I. Uddin, A. Jaiswal and P. Poddar, *International Journal of Innovative Biological Reaserch*, 2013, 2, 1-5.

14. M. Batic, D. Lenaracic, J. Stupar and P. Raspor, *Journal of Rapid Methods and Automation in Microbiology*, 1996, 4, 265-278.

15. V. Stehlik-Tomas, V. Zetic, D. Stanzer, S. Grba and N. Vahcic, *Food Technology and Biotechnology*, 2004, 42, 115-120.

16. D. Botstein, S. A. Chervitz and J. M. Cherry, *Science*, 1997, 277, 1259-1260.

17. P. E. Hodges, W. E. Payne and J. I. Garrels, *Nucleic Acids Research*, 1998, 26, 68-72.

18. Biotechnology Program under the Toxic Substances Control Act (TSCA), Saccharomyces cerevisiae Final Risk Assessment, http://www.epa.gov/biotech_rule/pubs/fra/fra002.htm.

19. S. Tenzer, D. Docter, J. Kuharev, A. Musyanovych, V. Fetz, R. Hecht, F. Schlenk, D. Fischer, K. Kiouptsi, C. Reinhardt *et al. Nat. Nanotechnol.,* 2013, 8, 772–781.

20. M. P. Monopoli, C. Aberg, A. Salvati, and K. A. Dawson, *Nat. Nanotechnol.,* 2012, 7, 779–786.

21. M. Kandpal, C. Sharan, P. Poddar, K. Prashanthi, P. R. Apte and V. Ramgopal Rao, *Applied Physics Letters*, 2012, 101, 104102.

22. S. Samuel M, L. Bose and George KC, *Academic Review*, 2009, 16, 57-65.

23. Y. Ma, *Journal of Wide Bandgap Materials*, 2002, 10, 113-120.

24. W. J. Huang, G. C. Fang and C. C. Wang, *Colloid Surface A*, 2005, 260, 45-51.

25. A. Khan and M. E. Kordesch, *Physica E,* 2005, 30, 51-54.

26. S. H. Ko, D. Lee, H. W. Kang, K. H. Nam, J. Y. Yeo, S. J. Hong, C. P. Grigoropoulos and H. J. Sung, *Nano Letters*, 2011, 11, 666-671.

27. K. Leschkies, R. Divakar, J. Basu, E. Enache-Pommer, J. Boercker, C. Carter, U. Kortshagen, D. Norris and E. Aydil, *Nano Letters*, 2007, 7, 1793-1798.

28. A. Martinson, J. Elam, J. Hupp and M. Pellin, *Nano Letters*, 2007, 7, 2183-2187.

29. N. K. Zayer, R. Greef, K. Rogers, A. J. C. Grellier and C. N. Pannell, *Thin Solid Films*, 1999, 352, 179-184.

30. M. Huang, S. Mao, H. Feick, H. Yan, Y. Wu, H. Kind, E. Weber, R. Russo and P. Yang, *Science*, 2001, 292, 1897-1899.

31. K. Vanheusden, W. L. Warren, C. H. Seager, D. R. Tallant, J. A. Voigt and B. E. Gnade, *Journal of Applied Physics*, 1996, 79, 7983-7990.

32. M. Willander, O. Nur, S. Zaman, a. Zainelabdin, N. Bano and I. Hussain, *Journal of Physics D: Applied Physics,* 2011, 44, 224017.

33. N. Salah, S. S. Habib, Z. H. Khan, A. Memic, A. Azam, E. Alarfaj, N. Zahed and S. Al-Hamedi, *International Journal of Nanomedicine*, 2011, 6, 863-869.

34. N. H. Cho, T. C. Cheong, J. H. Min, J. H. Wu, S. J. Lee, D. Kim, J. S. Yang, S. Kim, Y. K. Kim and S. Y. Seong, *Nature Nanotechnology*, 2011, 6, 675-682.

35. C. Hanley, J. Layne, A. Punnoose, K. Reddy, I. Coombs, A. Coombs, K. Feris and D. Wingett, *Nanotechnology*, 2008, 19, 295103.

36. S. Rani, P, Suri, P. K. Shishodia, and R.M. Mehra, *Solar Energy Materials and Solar Cells*, 2008, 92, 1639-1645.

37. Y. Ni, X. Cao, G. Wu, G. Hu, Z. Yang and X. Wei, *Nanotechnology*, 2007, 18, 155603.

38. S. Polarz, A. Roy, M. Merz, S. Halm, D. Schröder, L. Schneider, G. Bacher, F. Kruis and M. Driess, *Small* (*Weinheim an der Bergstrasse, Germany*), 2005, 1, 540-592.

39. N. Yong-hong, W. Xian-wen, H. Jian-ming and Y. Yin, *Materials Science and Engineering: B*, 2005, 121, 42-47.

40. N. Yonghong, Y. Sen, H. Jianming, Z. Peng, Z. Yunyou and C. Daobao, *Scripta Materialia*, 2008, 59, 127-130.

41. S. Mahpeykar, J. Koohsorkhi and H. Ghafoori-Fard, *Nanotechnology*, 2012, 23, 165602.

42. A. Jain, R. Bhargav and P. Poddar, *Materials Science and Engineering C*, 2013, 33, 1247-1253.

43. A. Demirci, A. L. Pometto, *Journal of Agricultural and Food Chemistry*, 1999, 47, 2491-2495.

44. A. R. Shet, L. R. Patil, V. S. Hombalimath, A. Deepak and B. B. Udapudi, *Biotechnology Bioinformatics and Bioengineering*, 2011, 1, 523-527.

45. E. Casals, T. Pfaller, A. Duschl, G. J. Oostingh and V. Puntes, *ACS Nano*, 2010, 4, 3623-3632.

46. U. Özgür, Y. I. Alivov, C. Liu, a. Teke, M. a. Reshchikov, S. Doğan, V. Avrutin, S.-J. Cho and H. Morkoç, *Journal of Applied Physics*, 2005, 98, 041301.

47. A. B. Djurisić and Y. H. Leung, *Small (Weinheim an der Bergstrasse, Germany)*, 2006, 2, 944-961.

48. E. Heftmann, *Chromatography, 5th Edition*.

49. A. K. Bhunia, P. K. Samanta, S. Saha and T. Kamilya, *Applied Physics Letters*, 2013, 103, 143701.

50. S. Dhara, P. K. Giri, *Applied Nanoscience*, 2011, 1, 165-171.

51. J. Weller, B. Dorfman, M. Soller and A. Friedmann, *Antonie Van Leeuwenhoek*, 1981, 47, 193-207.

52. C. Simm, B. Lahner, D. Salt, A. LeFurgey, P. Ingram, B. Yandell and D. J. Eide, *Eukaryotic Cell*, 2010, 6, 1166-1177.

53. D. J. Eide, *Biochemica et Biophysica Acta*, 2006, 1763, 711-722.

Figures

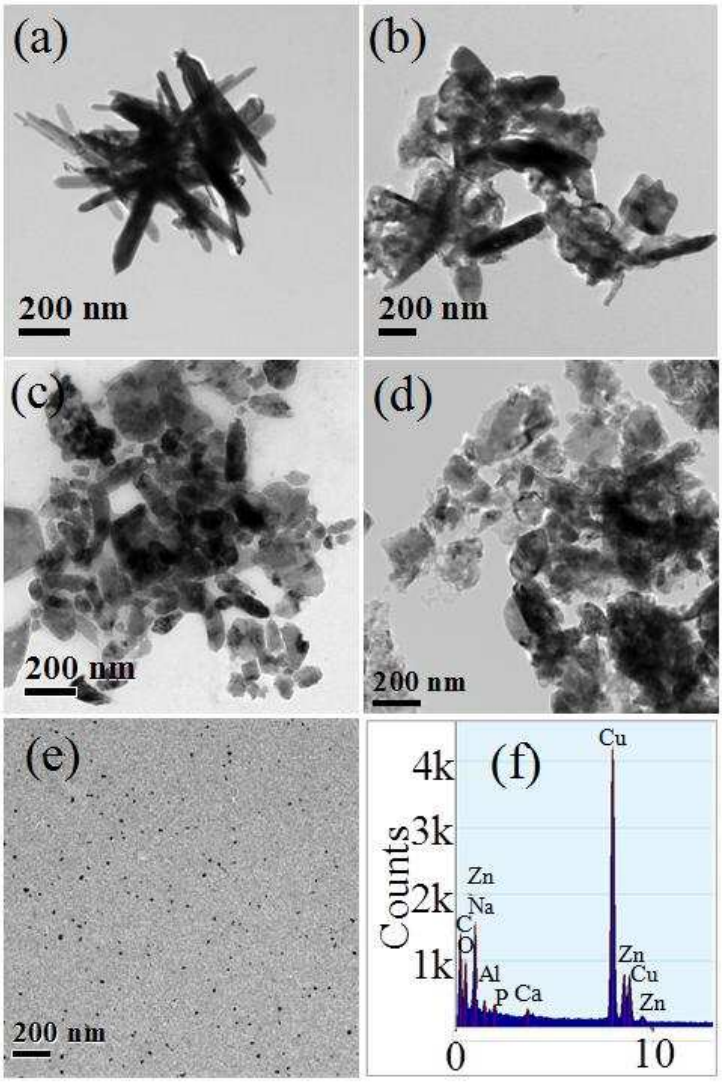

Figure 1. TEM images showing the different stages of biomilling of the rod-shaped ZnO NPs. (a-e) TEM images of ZnO NPs at 0 h, 24 h, 72 h, 120 h and 168 h of biomilling, respectively. (f) EDS result demonstrates the presence of zinc in sample at 168 h.

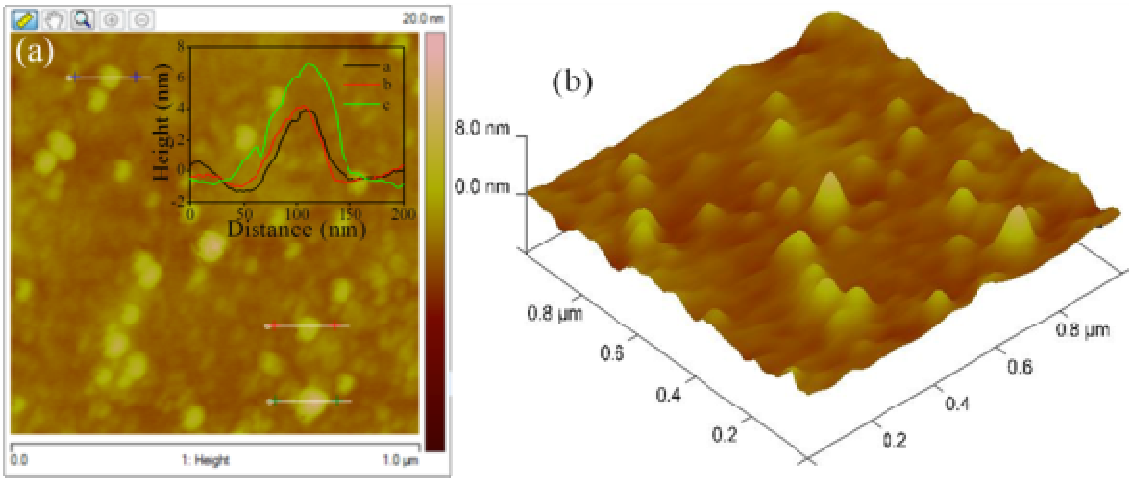

Figure 2. (a) AFM height image showing the presence of quasi-spherical ZnO NPs after 168 h of biomilling and (b) its 3D view.

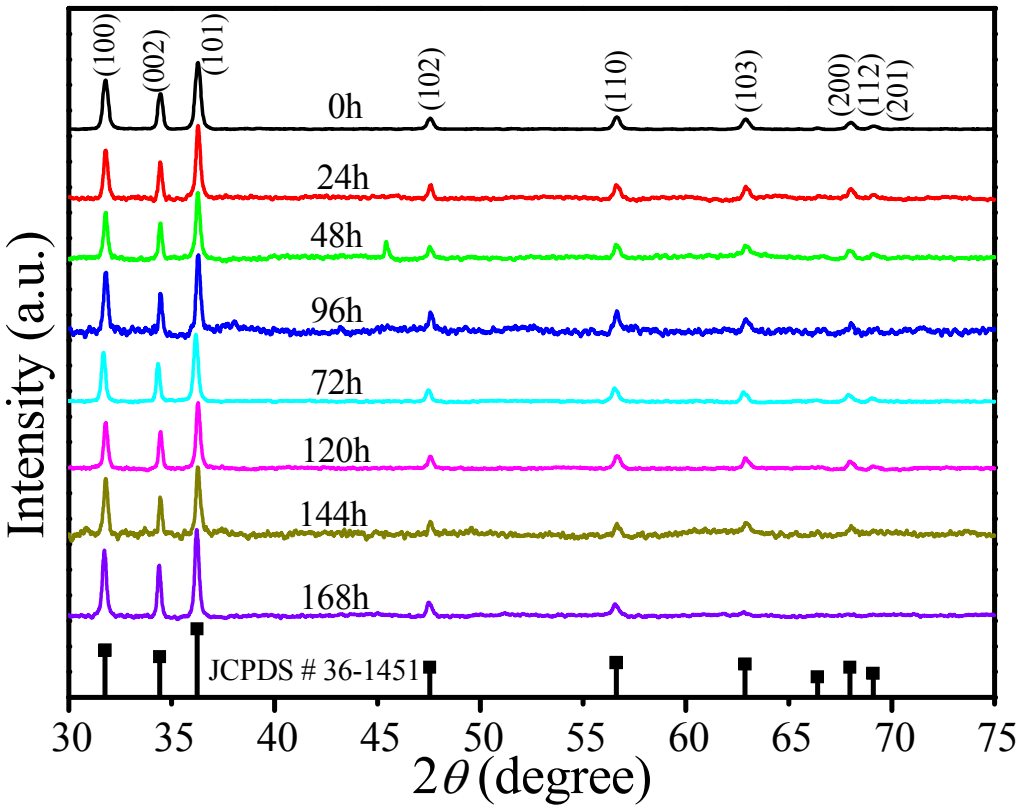

Figure 3. XRD patterns of ZnO NPs at different stages (0, 24, 48, 72, 96, 120, 144 and 168 h) of biomilling. The XRD profile was indexed to the PDF card no 36-1451 represented by black vertical lines.

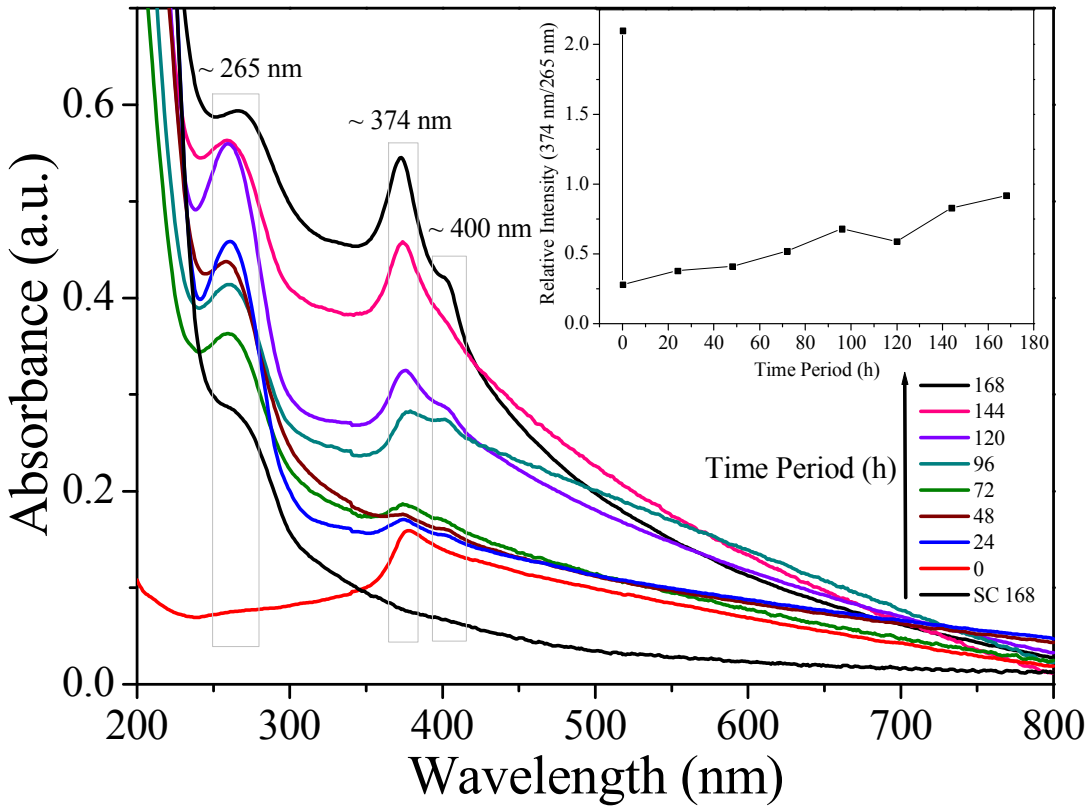

Figure 4. A comparison of UV-visible spectra between the ZnO NPs at different stages of biomilling (0, 24, 48, 72, 96, 120, 144 and 168 h) and supernatant of *S. cerevisiae* culture after 168 h (without ZnO NPs, as negative control).

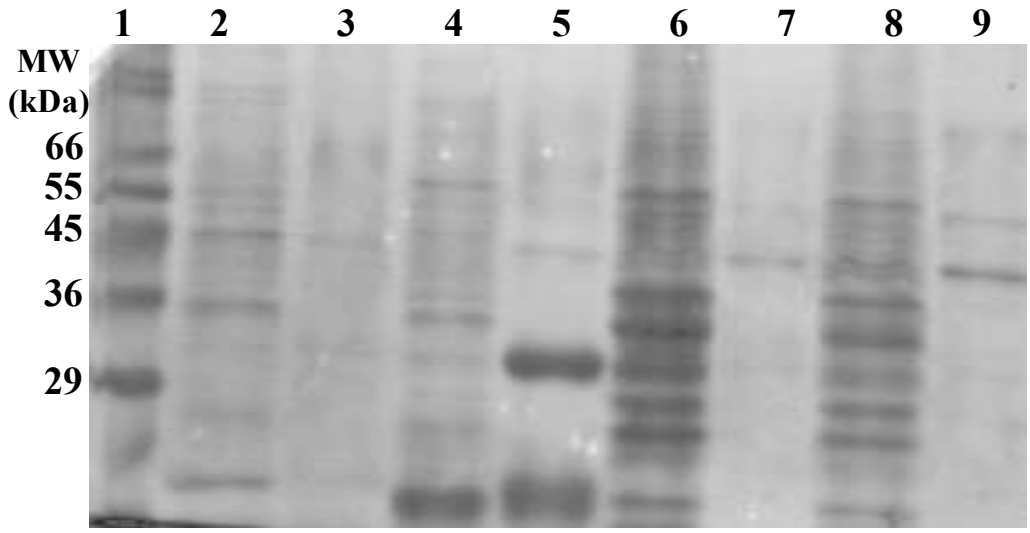

Figure 5. SDS-PAGE data showing the extracellular protein expression profile. Column 1 shows marker protein bands ~ 66, 55, 45, 36 and 29 kDa from top to bottom. Columns 2, 4, 6, 8 are for control samples and columns 3, 5, 7, 9 are for test samples after 24, 72, 120 and 168 h, respectively.

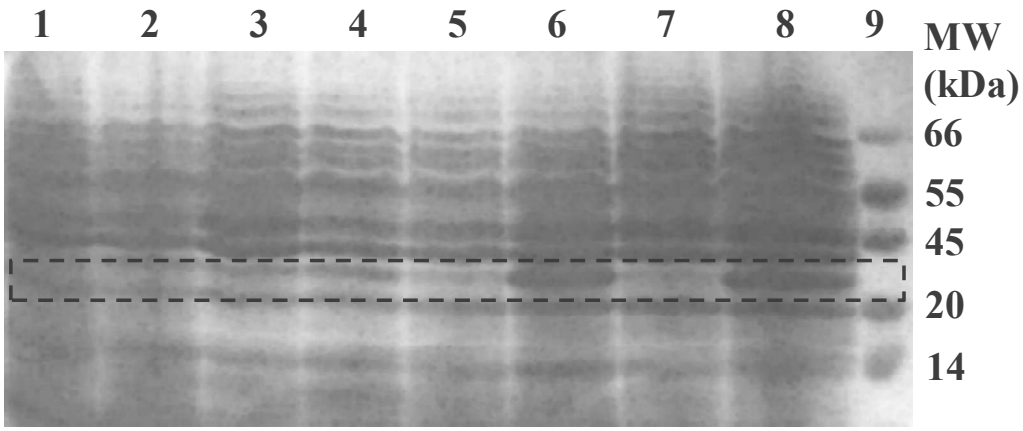

Figure 6. SDS-PAGE data showing the intracellular protein expression profile. Columns 1, 3, 5, 7 show control samples and columns 2, 4, 6, 8 are for test samples after 24, 72, 120 and 168 h biomilling, respectively. Column 9 shows marker protein bands ~ 66, 55, 45, 20 and 14 kDa from top to bottom.

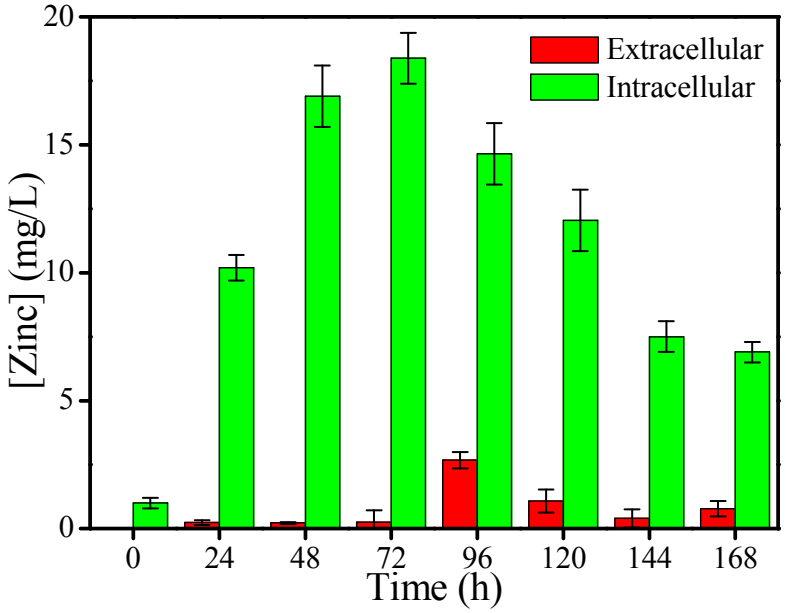

Figure 7. The extracellular (red color) and intracellular (green color) zinc content at different stages (24, 48, 72, 96, 120, 144 and 168 h) of biomilling.

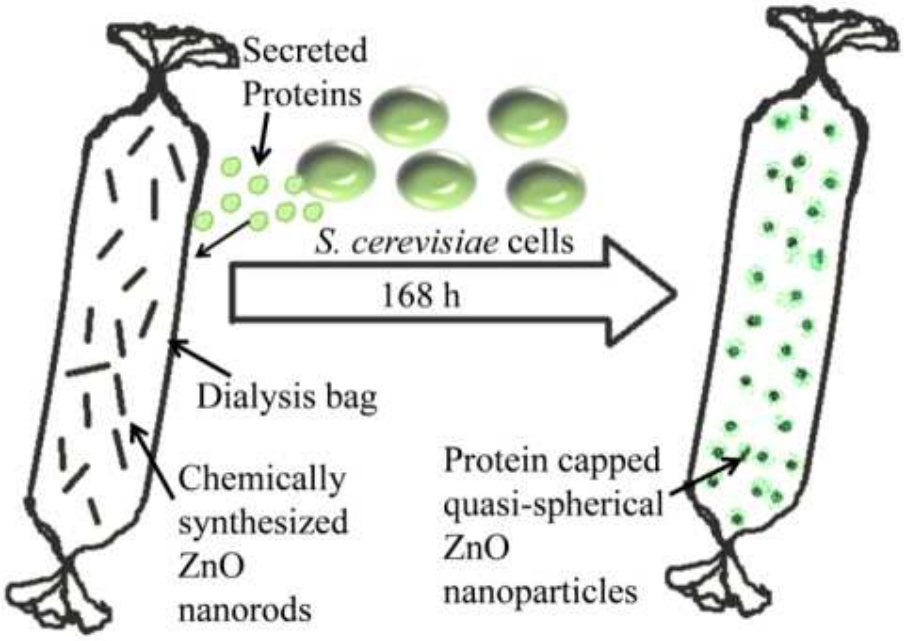

Scheme 1. Mechanism of transformation of chemically synthesized positively charged ZnO NRs to the protein-capped negatively charged quasi-spherical ZnO NPs after ~ 168 h of biomilling; a potential role of protein corona secreted by *S. cerevisiae* cells.

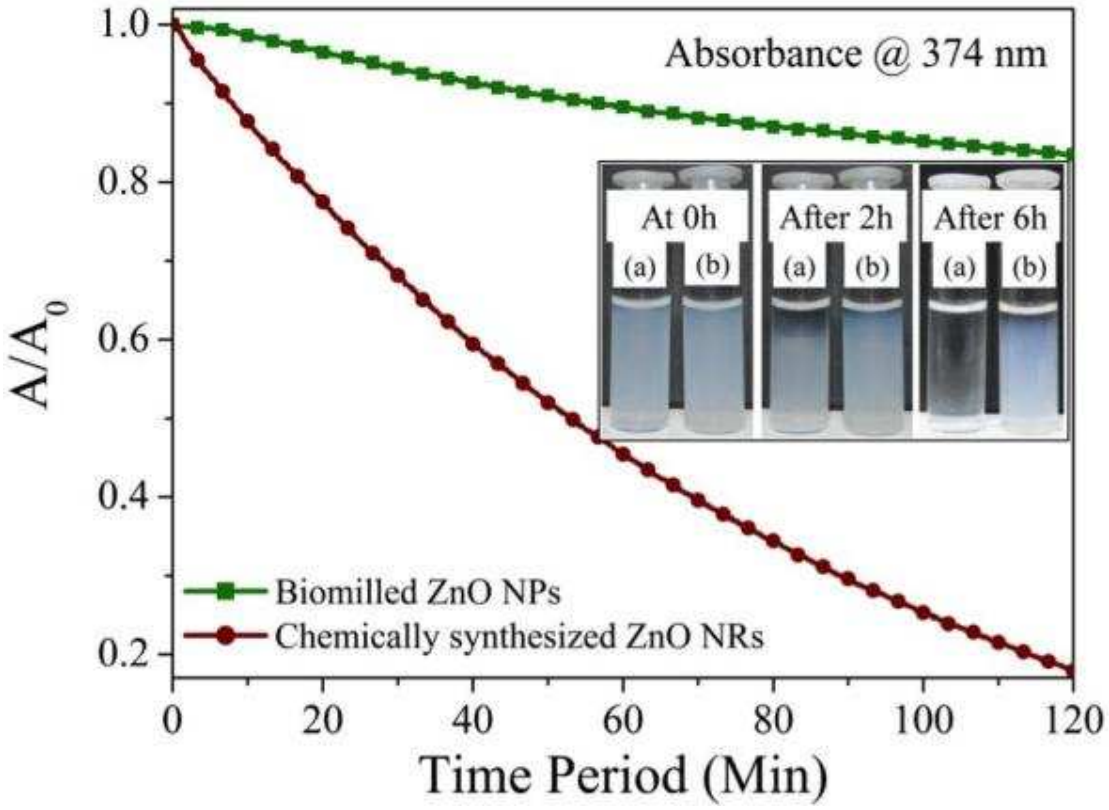

Figure 8. Dispersibility of the ZnO NPs in an aqueous medium as a function of time. Inset shows the stability of (a) the chemically synthesized ZnO NPs and (b) the biomilled ZnO NPs in aqueous suspension at different time periods of 0 h, 2 h and 6 h.

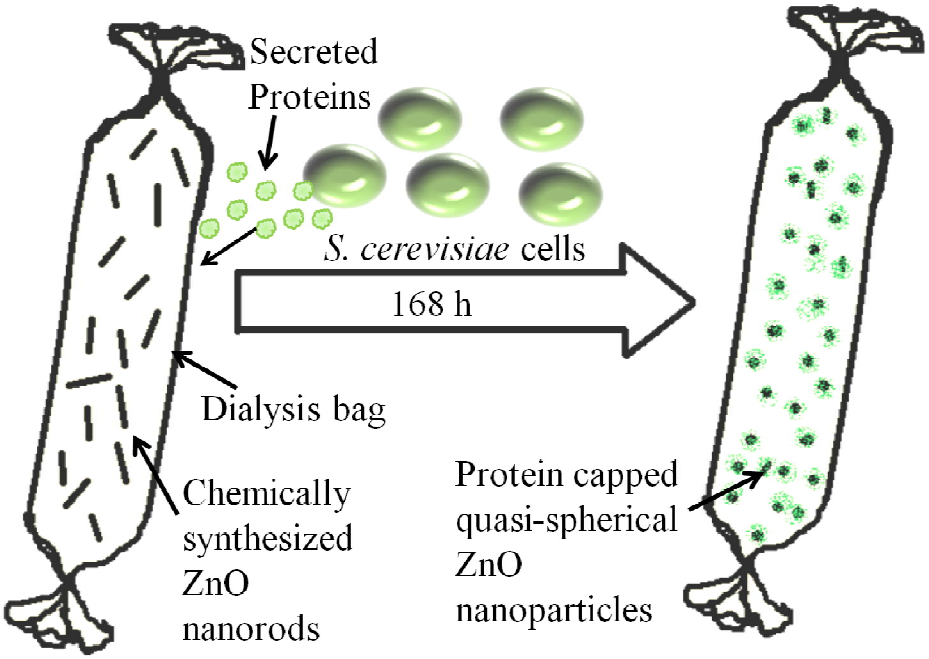

Break-down of chemically synthesized ZnO nanorods to small quasi-spherical ZnO NPs possibly due to the proteins secreted by *Saccharomyces cerevisiae*.